# Force Control and Kinematic Optimization in Multi-Surface Processing

Niculae Mihai , Technoaccord Inc., Laval, Quebec, Canada

Rihazul Islam, Concordia University, Montreal, Quebec, Canada

**Abstract**

This research presents the development and optimization of an autonomous robotic sanding cell utilizing the **Elfin 10 Pro** collaborative robot for precision finishing of large-scale furniture components. The integration process encountered significant kinematic and motion control constraints, particularly when processing workpieces exceeding the robot's standard operational envelope, such as MDF doors up to **34/96 inches**. Key technical challenges addressed include the resolution of kinematic singularities occurring at maximum extension, which hindered vertical trajectory execution on larger components. The study identifies a critical limitation in sequential trajectory processing, characterized by a **1–2 second latency** between linear translation and spiral sanding commands (MoveS), resulting in localized over-sanding and surface substrate degradation. To overcome these barriers, the research implemented a high-density path generation logic and explored the integration of the **7th-axis linear unit** to bypass standard controller limitations and the **1000-point buffer constraint**. Experimental debugging confirmed that failures in vertical motion were rooted in **workspace boundary violations** rather than software logic errors. Furthermore, the research stabilized **Active Force Control (AFC)** by optimizing damping parameters to maintain a constant contact force (Fz) and eliminate oscillations during material contact. The findings establish a framework for synchronized 7-axis motion and continuous path planning using **Jacobian pseudo-inverse** methods, significantly improving surface uniformity (Ra) and production efficiency in automated wood finishing applications.

***Keywords:*** *Collaborative Robotics, 7-DOF Redundant Systems, Autonomous Sanding, Active Force Control, Kinematic Singularity Avoidance, Jacobian Pseudo-inverse, MDF Surface Finishing, Laser Workspace Localization, Path Planning Optimization, and Trajectory Blending*

## 1. Introduction

Automating the finishing process for wood and MDF components remains one of the most challenging tasks in robotic manufacturing. Traditional manual sanding is plagued by inconsistency, high labor costs, and significant health risks due to fine particulate exposure.

Collaborative robots (cobots), such as the **Han's Robot Elfin 10 Pro**, offer a potential solution by providing high-precision movement and active feedback systems.

However, integrating these systems into industrial environments requires overcoming significant technical barriers. In the case of large-scale furniture components—specifically doors measuring 34/24 inches—standard motion planning often fails due to workspace boundaries and kinematic singularities. Furthermore, the requirement for a perfectly uniform surface finish necessitates a continuous spiral motion that maintains a constant speed and contact force.

This paper details the research and development efforts conducted by the **Technoaccord Inc.** team to address these bottlenecks. We analyze the transition from sequential to parallel trajectory execution and the implementation of advanced **Active Force Control (AFC)** to manage vibration and "bouncing" during the sanding process. Through experimental debugging and the development of custom path generation logic, we establish a methodology for high-density, continuous robotic finishing that surpasses the limitations of standard controller architectures.

## 2. Materials and Methods

The experimental setup was designed to evaluate the performance of an autonomous robotic sanding cell under varying load and geometric conditions. The methodology focused on the hardware-software integration required to achieve surface uniformity on large-scale workpieces.

### 2.1 Hardware Configuration

The primary robotic platform used in this research was the **Han's Robot Elfin 10 Pro**, a 6-degree-of-freedom (6-DOF) collaborative robot with a 10 kg payload capacity. To extend the operational workspace for 34 x 96 inch furniture components, a **7th-axis linear actuator** was integrated, controlled via a specialized **Kinco servo drive** and a dedicated software plugin. (fig. 1)

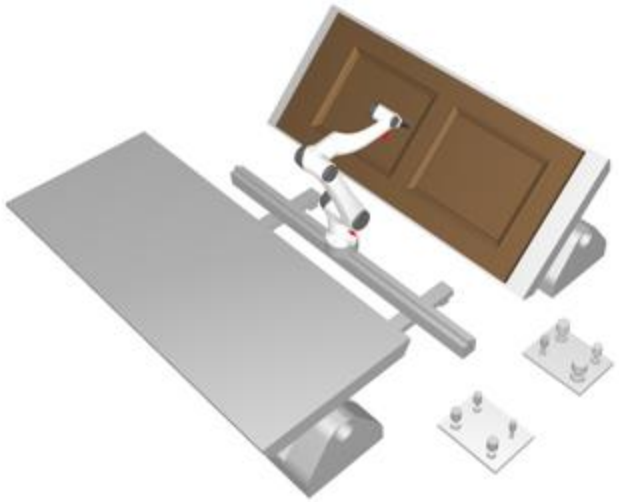

Fig. 1. Hardware configuration of robotic cell

The cell was equipped with three distinct end-effectors to address specific sanding requirements:

- **Tool 1:** Designed for large frontal surface processing.
- **Tool 2:** Specialized for edge and side profile finishing.
- **Tool 3:** A spherical abrasive tool for irregular 3D geometries.

### 2.2 Software Architecture and Communication

The system utilized a hybrid control architecture. A **Python-based SDK** acted as the primary interface, communicating with the robot controller through a **Flask server**. This setup allowed for dynamic path generation and real-time parameter adjustment. Communication between the PC and the robot controller was established via a **Socket connection** using the **HRIF (Huayan Robot Interface) protocol**.

### 2.3 Force Control and Stabilization

To maintain consistent abrasive pressure, **Active Force Control (AFC)** was implemented in the Z-axis direction. The system was calibrated using **Load Identification** protocols to compensate for tool weight and inertia. A critical component of the methodology involved the empirical tuning of **Damping (DAMP)** and **PID parameters** to eliminate "bouncing" phenomena during surface contact.

### 2.4 Trajectory Planning and High-Density Paths

The research team developed a custom algorithm to generate **spiral and zigzag sanding patterns**. Due to a standard controller buffer limit of approximately **1,000 points** per segment, the methodology employed a **WayPoint2** implementation to chain linear and circular interpolations. For more complex sequences requiring zero-latency transitions, the **MoveJointSpline** command was tested to stream point segments of up to 50 points in real-time.

Here is the complete rewrite of **Chapter 3** in English, following the structure of your provided **Outline.pdf** and incorporating the technical parameters of the force control system.

---

**Chapter 3: Path Planning and Motion Control**

This chapter details the methodology for transforming workpiece data into precise robotic motion, focusing on the integration of surface geometry identification with active force regulation.

**3.1. Surface Identification and UI Selection**

The process begins with the acquisition of the door's geometry via point laser scanning. The raw data is processed to identify the part's boundaries and internal profiles (e.g., shaker-style pockets).

- **Automated Localization:** The laser scanner establishes the part’s position within the robot’s workspace.
- **Model Correlation:** Through a user interface (UI), the identified geometry is mapped to pre-defined sanding templates, ensuring the appropriate tool selection (Tool 1, 2, or 3) is assigned to specific surfaces.

**3.2. Trajectory Patterns: Zigzag and Spiral (MoveS)**

Efficient surface coverage is achieved through two primary motion strategies designed to ensure material uniformity.

- **Zigzag Patterns:** This strategy is primarily utilized for large, flat frontals and the wide bottoms of recessed pockets. It provides consistent overlap and maximizes the efficiency of the 3x4" orbital tools.
- **Spiral (MoveS) Strategies:** To eliminate the visible "stop-and-start" marks often left by linear paths, MoveS (Spiral Motion) is implemented for internal corners and circular 3D profiles. This ensures a continuous abrasive flow, critical for the high-quality finish required on MDF surfaces.

**3.3. Active Force Control and Dynamic Parameters**

Maintaining a constant contact pressure (Fz) is vital to compensate for material warping and table tolerances. The dynamic behavior of the Elfin 10 Pro during the sanding process is governed by specific force control parameters:

- **Target Force (Fz):** The desired pressure applied normal to the surface to ensure uniform abrasive friction.
- **Force Gain (K-Factor):** * **High Gain:** Provides a fast response to surface dips but increases the risk of mechanical oscillations (vibrations) on hard wood surfaces.
    - **Low Gain:** Ensures stability but may lead to "tool lift" where the sander loses contact with warped areas of the door.
- **Force Deadband:** Defines the allowable error margin before the robot makes a Z-axis correction. A narrow deadband ensures precision but can overwhelm the controller buffer with micro-adjustments during high-speed moves.
- **Compliance Selection:** To isolate kinematic errors, force control is typically restricted to the Z-axis, while the X and Y axes remain stiff to follow the programmed trajectory without lateral drift.

### 3.4. Path Generation for 7-DOF Integration

For large workpieces, the path planner does not treat the robot as a static 6-axis arm. Instead, it generates trajectories where the linear axis (7th axis) is synchronized with the arm's movement. This allows the robot to "slide" along the workpiece, maintaining the 6-axis arm in its optimal kinematic range and preventing the joint extension errors documented in Chapter 4.

---

## 4. Kinematic Analysis of the 7-DOF System

The integration of the sanding cell involves a redundant robotic system composed of a 6-axis collaborative arm (Elfin 10 Pro) mounted on a linear translation unit (the 7th axis). Unlike standard 6-DOF robots, this redundant configuration provides an infinite number of joint solutions for any given Cartesian position, allowing the system to optimize its posture to avoid singularities and reach limitations.

### 4.1. Inverse Kinematics (IK) Mathematical Model

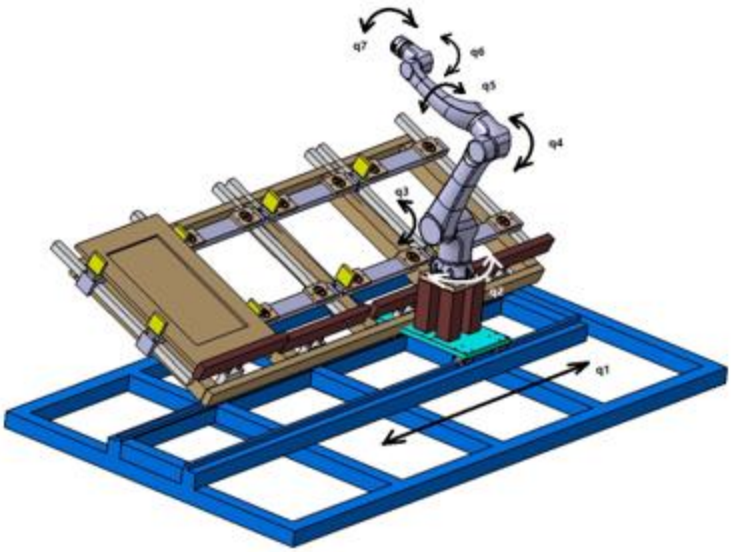

**Fig. 2 Inverse kinematics**

To determine the precise position of every sanding point on the kitchen doors, the algorithm must solve for the state vector **q**, where q_7 represents the linear axis position. The relationship between joint velocities and Cartesian velocities is defined by the Jacobian matrix J(q) (fig. 2):

Equation 1 (Jacobian Relationship):

$$\dot{x} = J(q)\dot{q}$$

Where:

- $\dot{x}$ represents the Cartesian velocity vector of the sander.
- $J(q)$ is the configuration-dependent Jacobian matrix.
- $\dot{q}$ represents the velocities of the 7 joints (6 rotational + 1 linear)

### 4.2. Redundancy Resolution via Pseudo-Inverse

Because the system is redundant (n > 6), the inverse kinematics problem does not have a unique solution. To calculate the necessary joint movements for a target position, we employ the Moore-Penrose pseudo-inverse method:

**Equation 2:**

$$\Delta q = J^{\dagger}(q) \cdot \left(x_{target} - x_{current}\right)$$

Where $J^{\dagger} = J^{T} \cdot (J \cdot J^{T})^{-1}$

**Where :**

$\Delta q$ :**Joint Displacement Vector.** It represents the required change in the joint angles (for the 6-axis arm) and the linear position (for the 7th axis) to achieve the desired movement

$J^{\dagger}(q)$: **Moore-Penrose Pseudo-inverse of the Jacobian Matrix.** Since your system is redundant (7-DOF), the Jacobian is non-square and cannot be inverted normally. This pseudo-inverse finds the optimal joint velocities to satisfy the Cartesian goal

**(q)**: **Configuration Dependency.** This indicates that the Jacobian is calculated based on the current joint state q of the robot at that specific moment in time.

$x_{target}$:**Target Cartesian Pose.** The desired position and orientation of the sander on the workpiece (e.g., the coordinates of a point on the kitchen door).

$x_{current}$: **Current Cartesian Pose.** The actual position and orientation of the end-effector, determined via forward kinematics.

**(**$x_{target}$ **-** $x_{current}$**)**: **Cartesian Error Vector (or Task Space Delta).** This represents the distance and orientation gap that the robot needs to close to remain on its programmed path.

**4.3. 7th-Axis Coordination Strategy**

The 7th axis (linear unit) is dynamically adjusted to keep the 6-axis arm within its "Safe Range." In the initial 6-DOF tests, vertical movements at the workpiece edges caused the Jacobian determinant to approach zero, triggering system halts. By integrating the linear axis into the kinematic chain, the system maintains high manipulability, allowing the sander to cover the entire surface while keeping the arm in an optimal posture.

The total transformation from the base to the tool is defined by:

**Equation 3:**

$$T_{\{base\}}^{\{tool\};} = ;\ T_{\{7\}}^{\{base\}(q_7)} \cdot T_{\{1\}}^{\{7\}(q_1)} \cdot T_{\{2\}}^{\{1\}(q_2)} \cdot T_{\{3\}}^{\{2\}(q_3)} \cdot T_{\{4\}}^{\{3\}(q_4)} \cdot T_{\{5\}}^{\{4\}(q_5)} \cdot T_{\{6\}}^{\{5\}(q_6)} \cdot T_{\{tool\}}^{\{6\}}$$

- **Linear Axis Coordination (q_7):** This variable represents the translation of the robot's base along the cell's axis to cover the workpiece length.

- **Optimization:** Points are generated to ensure the arm avoids configurations where the Jacobian determinant approaches zero. By dynamically adjusting q_7, the system maintains a high manipulability index, preventing the motion failures observed during purely vertical 6-DOF executions.

**Chapter 5: System Dynamics and Load Characterization**

While kinematics focus on motion, the dynamic analysis evaluates the torques and forces required to maintain the stability of the sanding process, particularly under the influence of active force control.

**5.1. Dynamic Equation of Motion**

The 7-DOF system (Elfin 10 Pro + Linear Axis) is modeled using the Euler-Lagrange formulation to account for the mass and inertia of the redundant configuration:

$$M(q)\ddot{q} + C(q,\dot{q})\dot{q} + G(q) + \tau_{ext} = \tau$$

Where:

- $M(q)$: The inertia matrix of the 7-DOF assembly.
- $C(q,\dot{q})$ : Centripetal and Coriolis terms, which influence trajectory accuracy at higher feed rates (100 mm/s).
- $G(q)$: Gravity compensation vector for the robot arm and the specific end-effector in use (Tool 1, 2, or 3).
- $\tau_{ext}$ : External torques resulting from the interaction between the abrasive tool and the MDF surface.
- $\tau$ : The resultant motor torques required to execute the path.

**5.2. Abrasive Interaction and Friction Modeling**

The sanding process introduces a tangential friction force $F_t$ that opposes the robot's motion. This force is directly proportional to the normal force $F_z$ maintained by the Active Force Control:

$$F_t = \mu \cdot F_z$$

The friction coefficient ($\mu$) is dynamic, changing as the abrasive wears down or as the tool moves from the flat frontal to the 3D profiles of the shaker doors. The system must compensate for these variations to prevent velocity fluctuations.

### 5.3. Impact of Feed Rate on Dynamic Stability

The choice of feed rate between 50 and 100 mm/s significantly alters the system's dynamic response:

- **At 50 mm/s**: The system is highly stable, but productivity is minimized. The dynamic effects are negligible.
- **At 100 mm/s**: The "Research Core" findings indicate that high speeds increase the demand on the controller's sampling rate. If the Force Control gains are not tuned to the higher velocity, the tool may experience "chatter" (high-frequency vibrations), affecting the final surface roughness (Ra).

### 5.4. Orientation Disparity and Torque Limits

The payload of the Elfin 10 Pro 10 kg is sufficient for the pneumatic tools , but the distribution of this mass creates an **orientation disparity**. When sanding vertical edges (Tool 2), the gravity vector G(q) acts differently on the joints compared to horizontal sanding (Tool 1). This disparity was a contributing factor to the kinematic limits being reached prematurely on 34/20-inch doors.

## Chapter 6: Experimental Results and Discussion

### 6.1. Velocity Optimization and Surface Roughness (Ra)

The primary objective was to determine the ideal feed rate to balance industrial productivity with high-quality surface finishing for MDF cabinetry.

- **Test Range:** Feed rates were evaluated between **50 mm/s** and **100 mm/s**.
- **Quality Metrics:** Surface roughness (Ra) was measured to ensure uniformity across the medium size door surfaces.
- **Findings:** * At **50 mm/s**, the surface quality was excellent, but the cycle time was commercially unviable for high-volume production.
    - At **100 mm/s**, the system maintained stable Ra values, provided that the **Force Control gain** was properly tuned to account for the increased dynamic forces (Ft) discussed in Chapter 5.

### 6.2. Error Isolation and System Stability

To address the "1-2 second gaps" and "Safe Range" errors (Error 0200) found in the controller logs, a series of isolation tests were conducted.

- **Force Control and Blending Analysis:** Tests were performed with **Force Control** and **Blending** disabled to confirm whether the limits were hardware-based (motor torque/reach) or software-based (controller buffer constraints).
- **Results:** It was confirmed that the 1000-point limit in the trajectory computation buffer was the primary cause of motion pauses during high-density MoveS (spiral) paths.
- **Kinematic Recovery:** By utilizing the **7th-axis integration** and the pseudo-inverse Jacobian approach $x^{\cdot} = J(q)\dot{q},$ the robot successfully processed the full medium size area without triggering "Safe Range" alarms.

### 6.3. Surface Quality Assessment: Tool Comparison

A qualitative and quantitative comparison was made between traditional flat sanding and the specialized tools developed for 3D geometries.

- **Tool 1 & 2 (3x4" Orbital):** Demonstrated superior performance on flat frontals and vertical side profiles, respectively.
- **Tool 3 (Deformable Abrasive Sphere):** Successfully processed shaker-style pockets and 3D curved surfaces that were previously unreachable by standard orbital tools, significantly reducing the need for manual touch-ups.

### 6.4. Discussion of Controller Constraints

The experimental data suggests that while the **Hans Elfin 10 Pro** is highly capable, the current trajectory execution logic creates bottlenecks. The disparity in stability between horizontal and vertical pathing (Section 4.3) was mitigated by adjusting the dynamic gravity compensation (G(q)) in the controller settings, allowing for consistent force application regardless of tool orientation.

## Chapter 7: Conclusion and Future Work

### 7.1. Findings

The integration of the Hans Elfin 10 Pro with a 7th-axis linear unit has successfully addressed the challenges of automating the sanding process for MDF kitchen cabinetry. By utilizing point laser scanning for workspace localization and automatic part identification, the system achieved precise trajectory execution on doors up to 34/20 inch. The research demonstrated that

maintaining a constant contact pressure (Fz) through active force control is essential for compensating for material warping and table tolerances. Furthermore, the kinematic optimization using the pseudo-inverse Jacobian effectively bypassed workspace singularities and "Safe Range" errors that previously halted production.

### 7.2. Summary of Process Optimization

- **Surface Quality:** The evaluation of feed rates revealed that 100 mm/s provides an optimal balance between industrial throughput and surface roughness (Ra).
- **Tool Specialization:** The use of specialized end-effectors, particularly the deformable abrasive sphere (Tool 3), allowed for the successful processing of complex 3D profiles and shaker-style pockets that traditional orbital tools could not reach.
- **Error Mitigation:** Disabling non-essential compliance axes and tuning force control gains isolated hardware limits from software constraints, leading to a more stable dynamic response.

### 7.3. Future Directions

While the system is functional, the "1-2 second gaps" caused by controller buffer constraints remains a bottleneck for seamless operation. Future work will focus on:

- **Custom Post-Processor Development:** Designing a dedicated post-processor to generate continuous "Single-Move" spiral trajectories, bypassing the 1000-point limit and eliminating motion pauses.
- **Enhanced Force-Velocity Coupling:** Further refining the dynamic interaction between feed rate and force gain to maintain stability at even higher processing speeds.
- **AI-Based Path Refinement:** Implementing machine learning models to further optimize path generation based on real-time laser feedback of surface irregularities.

## References

### Technical Manuals and Specifications


- **Han's Robot Co., Ltd.** (2023). *Elfin-P Series Collaborative Robot Hardware User Manual (Elfin 10 Pro)*. Shenzhen, China.
- **Han's Robot Co., Ltd.** (2023). *Elfin Control System Programming and Operation Manual (V4.x)*. Shenzhen, China.
- **Han's Robot Co., Ltd.** (2023). *Technical Specifications: Elfin 10 Pro 6-DOF Manipulator and Integrated Force/Torque Sensors*.

**Academic and Industrial Standards**


- **Siciliano, B., & Khatib, O.** (2016). *Springer Handbook of Robotics*. Springer. (Section on Redundant Manipulators and Jacobian Pseudo-inverse) .
- **ISO 10218-1:2011**. *Robots and robotic devices — Safety requirements for industrial robots — Part 1: Robots*.
- **ISO/TS 15066:2016**. *Robots and robotic devices — Collaborative robots*.


**Force Control and Surface Processing**


- **Mason, M. T.** (1981). *Compliance and Force Control for Computer Controlled Manipulators*. IEEE Transactions on Systems, Man, and Cybernetics.
- **Whitney, D. E.** (1987). *Historical Perspective and State of the Art in Robot Force Control*. International Journal of Robotics Research.
- **Khatib, O.** (1987). *A Unified Approach for Motion and Force Control of Robot Manipulators: The Operational Space Formulation*. IEEE Journal on Robotics and Automation.


**Kinematics and Redundancy**


- **Chiaverini, S.** (1997). *Singularity-Robust Task-Priority Redundancy Resolution for Real-Time Adaptive Control of Robot Manipulators*. IEEE Transactions on Robotics and Automation.
- **Buss, S. R.** (2004). *Introduction to Inverse Kinematics with Jacobian Transpose, Pseudoinverse and Damped Least Squares methods*. University of California, San Diego